J Physiol 591.14 (2013) pp 3525–3538

The Journal of Physiology

Temporal and spatial distribution of Nrf2 in rat brain following stroke: quantification of nuclear to cytoplasmic Nrf2 content using a novel immunohistochemical technique

Salil Srivastava, Alessio Alfieri, Richard C. M. Siow, Giovanni E. Mann and Paul A. Fraser

Cardiovascular Division, British Heart Foundation Centre of Research Excellence, School of Medicine, King's College London, 150 Stamford Street, London SE1 9NH, UK

Key points

- The redox-sensitive transcription factor NF-E2 related factor 2 (Nrf2) plays a key role in regulating adaptive cellular antioxidant defences, and activation of Nrf2 in stroke protects the brain against oxidative stress following ischaemia-reperfusion injury.
- We report the first measurements of temporal and spatial distribution of Nrf2 in nuclear and cytoplasmic compartments in cells in the ischaemic core, peri-infarct regions and contralateral hemisphere of rat brain following cerebral ischaemia-reperfusion injury for 4, 24 or 72 h using a novel quantitative immunohistochemical technique, which was further validated in cultured bEnd.3 murine brain endothelial cells.
- Nrf2 expression in brain sections was increased in core and peri-infarct regions after 24 h reperfusion, with levels remaining elevated only in peri-infarct regions after 72 h. Pretreatment of rats with the Nrf2 inducer sulforaphane reduced core and peri-infarct Nrf2 levels after 24 h reperfusion.
- The time course of stroke-induced changes in nuclear to cytoplasmic Nrf2 content and its modulation by pretreatment with sulforaphane provide novel insights for targeting endogenous redox sensitive antioxidant pathways to ameliorate the damaging consequences of stroke.

Abstract Activation of the redox-sensitive transcription factor NF-E2 related factor 2 (Nrf2) affords protection against cerebral ischaemia-reperfusion injury via the upregulation of anti-oxidant defence genes. We have quantified for the first time Nrf2 content in brains from rats subjected to stroke and from cultured bEnd.3 brain endothelial cells using a novel immuno-histochemical technique. Male Sprague-Dawley rats were subjected to middle cerebral artery occlusion for 70 min followed by reperfusion for 4, 24 or 72 h. Coronal brain sections were incubated with anti-Nrf2 primary and biotinylated-horseradish peroxidase-conjugated secondary antibody, after which sections were reacted with 3,3′-diaminobenzidine (DAB) in the presence of hydrogen peroxide. The initial rates of DAB polymer formation were directly proportional to the Nrf2 protein concentration. Image processing was used to determine the temporal and spatial distribution of Nrf2 in nuclear and cytoplasmic compartments in stroke-affected and contralateral hemispheres. Nuclear to cytoplasmic Nrf2 ratios were increased in the stroke region after 24 h reperfusion and declined after 72 h reperfusion. Pretreatment with the Nrf2 inducer sulforaphane reduced total cellular Nrf2 levels in peri-infarct and core regions of the stroke hemisphere after 24 h reperfusion. Treatment of cultured murine brain endothelial cells with

*G. E. Mann and P. A. Fraser are joint senior authors.

DOI: 10.1113/jphysiol.2013.257964

sulforaphane (2.5 μM) increased nuclear accumulation of Nrf2 over 1–4 h. We report the first quantitative measurements of spatial and temporal nuclear Nrf2 expression in rat brains following stroke, and show that sulforaphane pretreatment affects Nrf2 distribution in the brain of naïve rats and animals subjected to cerebral ischaemia. Our findings provide novel insights for targeting endogenous redox-sensitive antioxidant pathways to ameliorate the damaging consequences of stroke.

(Resubmitted 1 May 2013; accepted 20 May 2013; first published online 20 May 2013)

Corresponding authors Dr P. A. Fraser and Prof. G. E. Mann: Cardiovascular Division, BHF Centre of Research Excellence, School of Medicine, King's College London, Franklin-Wilkins Building, 150 Stamford Street, London SE1 9NH, UK. Email: paul.fraser@kcl.ac.uk; giovanni.mann@kcl.ac.uk

Abbreviations ARE, antioxidant response element; BSA, bovine serum albumin; DAB, 3,3′-diaminobenzedine; DAPI, 4′,6-diamidino-2-phenylindole; GFAP, glial fibrillary acidic protein; HO-1, heme oxygenase-1; HRP, horseradish peroxidise; Keap1, Kelch-like associated protein 1; MCAo, middle cerebral artery occlusion; NQO1, NAD(P)H quinine oxidoreductase 1; Nrf2, NF-E2 related factor 2; PBS, phosphate-buffered saline.

Introduction

Brain damage following ischaemic stroke is the result of a series of pathophysiological mechanisms (Dirnagl *et al.* 1999; Candelario-Jalil, 2009), including an excess production of reactive oxygen species and reactive nitrogen species, with severe consequences for the viability of cells critical for brain function and cerebrovascular permeability (Alfieri *et al.* 2011; Chen *et al.* 2011; Fraser, 2011; Woodfin *et al.* 2011). The brain is at an increased risk of oxidative damage due its high demand for oxygen, high metabolic activity, increased content of unsaturated fatty acids and low intracellular antioxidant capacity (Shohami *et al.* 1997; Ozkul *et al.* 2007; Ikonomidou & Kaindl, 2011). The adverse neurological consequences following ischaemic stroke are initiated in the early hours after the onset of ischaemia (Thompson *et al.* 1999; Kolominsky-Rabas *et al.* 2006). Treatment strategies targeting endogenous repair mechanisms in the brain are now a prime focus of stroke research (Alfieri *et al.* 2011; Iadecola & Anrather, 2011).

The redox-sensitive transcription factor NF-E2 related factor 2 (Nrf2) orchestrates endogenous antioxidant defences against oxidative and nitrosative stress via the upregulation of phase II detoxifying enzymes and anti-oxidant stress proteins (Ishii *et al.* 2000). Under physiological conditions Nrf2 is bound by its cytoplasmic repressor Kelch-like associated protein 1 (Keap1) and targeted for proteasomal degradation (Motohashi & Yamamoto, 2004; Itoh *et al.* 2010; Taguchi *et al.* 2011). Oxidative and electrophilic stress induce nuclear translocation and binding of Nrf2 to the antioxidant response element (ARE) in the promoter of protective genes such as heme oxygenase 1 (HO-1), NAD(P)H:quinine oxidoreductase 1 (NQO1), peroxiredoxin 1 (Prx1) and γ-glutamyl cysteine ligase (Ishii *et al.* 2000, 2004; Motohashi & Yamamoto, 2004; Taguchi *et al.* 2011; Chapple *et al.* 2012). Activation of this pathway increases total protein expression and nuclear levels of Nrf2 (Kwak *et al.* 2002).

Although activation of Nrf2 has been reported to attenuate brain damage and neurological deficits following stroke (Shah *et al.* 2007; Yang *et al.* 2009; Alfieri *et al.* 2011; Kam *et al.* 2011; Tanaka *et al.* 2011), there are no reports that have quantified temporal and spatial distribution of Nrf2 in nuclear and cytoplasmic compartments of cells in the ischaemic core, peri-infarct regions and contralateral hemisphere following transient ischaemia-reperfusion injury. Moreover, the effects of pre-treatment of rats *in vivo* with sulforaphane, a known Nrf2 inducer contained in cruciferous vegetables (Zhang *et al.* 1992; Dinkova-Kostova & Kostov, 2012), on intracellular distribution of Nrf2 following stroke has to our knowledge not been reported.

Immunohistochemistry using 3,3′-diaminobenzidine (DAB) is a widely employed technique for studying the expression of proteins in tissues (Graham & Karnovsky, 1966). To date, application of this technique has only provided a semi-quantitative, pixel-by-pixel measure of the intensity of staining (Toyokuni *et al.* 1997; Matkowskyj *et al.* 2000). Formation of the coloured DAB polymer is dependent upon the number of horseradish peroxidase (HRP) active sites available to enzymatically oxidise DAB in the presence of hydrogen peroxide (Nakane & Pierce, 1967). Notably, the number of HRP active sites available to catalyse the oxidation of DAB is dependent upon the concentration of a given protein within the sample (Gauden *et al.* 2007). Thus, evaluation of the rate of DAB polymer formation allows for a more accurate quantification of protein content within nuclear and cytoplasmic compartments of cells in a given tissue sample.

In this study we have developed and validated a novel DAB-based immunohistochemical technique to quantify the temporal and spatial distribution of Nrf2 in nuclei and cytoplasmic compartments in brain sections *ex vivo* obtained from rats subjected to transient middle

cerebral artery occlusion (MCAo) and reperfusion injury. Simultaneous application of DAB and fluorescence immunohistochemical techniques enabled us to define nuclear to cytoplasmic distribution of Nrf2 and total cellular Nrf2 levels in core and peri-infarct regions of stroke-affected and contralateral brain hemispheres after 4, 24 and 72 h reperfusion. We further quantified the time course of nuclear to cytoplasmic distribution of Nrf2 in the mouse-derived brain endothelial cell line b.End3 challenged acutely with sulforaphane. We report the first quantitative measurements of temporal and spatial Nrf2 distribution in the brain following experimental stroke and further demonstrate that treatment of naïve animals with sulforaphane elevates Nrf2 levels in the brain, whilst pretreatment with sulforaphane prior to stroke reduces Nrf2 content in peri-infarct regions after 24 h reperfusion.

Methods

Materials

Porcine gelatine, bovine serum albumin (BSA), rabbit anti-BSA antibody, ascorbic acid and D,L-sulforaphane were purchased from Sigma (Gillingham, Dorset, UK). Rabbit anti-Nrf2 and donkey anti-goat Cy5 were purchased from Abcam (Cambridge, UK); donkey anti-mouse Alexafluor 555 (Invitrogen, Paisley, UK); 4′,6-diamidino-2-phenylindole (DAPI; Roche, Welwyn Garden City, UK); Bloxall endogenous peroxidase solution, Avidin and Biotin blocking solution, goat anti-rabbit biotinylated secondary antibody (Vectastain ABC elite kit), DAB and hydrogen peroxide (H_2O_2) substrate kit were purchased from Vector Laboratories Ltd (Peterborough, UK). Dulbecco's modified Eagle's medium (DMEM) containing 5.5 mM D-glucose and supplemented with 10% fetal calf serum, 4 mM L-glutamine and penicillin/streptomycin (100 IU ml^{-1}) was from Sigma.

Animals

Male Sprague-Dawley rats (weighing 250–300 g; Harlan, UK) were acclimatized for at least 1 week before surgery and maintained on a 12 h light/dark cycle. All procedures were performed under the authority of Project Licence No. PPL70/6579, in accordance with the UK Animal (Scientific Procedures) Act 1986 and rigorous ethical review process by the UK Home Office and King's College London.

Middle cerebral artery occlusion

Cerebral ischaemia was induced by transient intraluminal occlusion of the right middle cerebral artery (MCAo) under 4% isofluorane anaesthesia (Modo *et al.* 2000). A silicone-coated filament was inserted from the carotid bifurcation and left in place for 70 min. At the end of the occlusion period, the intraluminal filament was removed to allow reperfusion. MCAo was confirmed by examining flexion of the contralateral forelimb by lifting of the tail and spontaneous asymmetric turning behaviour. To examine the effects of activating Nrf2 *in vivo*, rats were pretreated with the Nrf2 inducer D,L-sulforaphane (5 mg kg^{-1} I.P., dissolved in 1% corn oil; Zhao *et al.* 2007; Benedict *et al.* 2012) 1 h before 70 min MCAo followed by 24 h reperfusion.

Removal of rat brains and coronal sectioning

Rats were killed with an overdose of pentobarbitone (120 mg kg^{-1} I.P.) following 4, 24 or 72 h reperfusion, and brains were then perfused with cold saline followed by 40 g l^{-1} paraformaldehyde in 0.1 M phosphate-buffered saline (PBS). After collection, fixed brains were left overnight in paraformaldehyde before being transferred to 300 g l^{-1} sucrose and stored at 4°C for subsequent sectioning. Coronal brain sections (10 μm) were cut on a cryostat (Bright, UK) onto Superfrost Plus glass slides (Thermo Scientific, UK; formal saline pretreated) and left to air dry for 48 h at room temperature. Sections were stored at −20°C for subsequent immunohistochemical and/or immunofluorescence analyses.

Immunohistochemical quantification of HRP covalently linked antibodies

The novel technique applied in this study extends our previous report, where HRP was used as a fluid phase marker to estimate blood–brain barrier permeability following ischaemia-reperfusion injury (Gauden *et al.* 2007). The principle that HRP can be measured in tissue sections from the initial rate of DAB polymer formation has been extended to quantify HRP covalently linked antibodies in *ex vivo* brain sections. In proof-of-principle experiments, we established that the relationship between conjugated secondary and primary antibodies and a target protein is essentially linear (Fig. 1). Known concentrations of BSA were dissolved in warm porcine gelatine 200 g l^{-1} solution and allowed to set at room temperature. The blocks, when set, were frozen, sectioned onto glass slides and fixed similarly to brain tissue (see below). Sections (10 μm) were incubated with rabbit anti-BSA at 4°C for 16 h, and then with a goat anti-rabbit biotinylated secondary antibody for 30 min at room temperature, followed by a further 30 min with the ABC reagent to amplify the DAB reaction product signal via the formation of the avidin and biotin complex. One section was taken from four replicate blocks for each albumin concentration, and regression coefficients calculated for the linear portion of each of

the optical density curves (see Fig. 1*A*). Figure 1*B* shows the relationship between the initial rate of DAB product development *versus* the BSA concentration in the gelatine blocks.

Preparation of brain sections for immunohistochemistry and antibody incubation

Brain sections were defrosted at room temperature following removal from −20°C and quenched for endogenous peroxidase activity using Bloxall (Vector Laboratories Ltd) for 10 min at room temperature. Sections were gently washed with PBS and incubated with avidin D for 15 min at room temperature, excess avidin D solution gently blotted off, and the section then incubated for a further 15 min at room temperature with biotin blocking solution (Vector Laboratories Ltd) according to the manufacturer's instructions. Brain sections were permeabilised with 1 g l^{-1} Triton-X 100 (Sigma) in PBS with 10% normal donkey serum and then incubated with primary antibodies goat anti-glial fibrillary acidic protein (GFAP, 1:400) and rabbit anti-Nrf2 (1:100) overnight at 4°C. GFAP was also identified by fluorescence, and sections incubated with secondary antibodies (donkey anti-goat Cy5, 1:500) for 1 h at room temperature.

To quantify Nrf2 by immunohistochemistry, brain sections were incubated with goat anti-rabbit biotinylated secondary antibody and ABC reagent to amplify the DAB reaction product signal. Brain sections were washed with doubly distilled water and stained with DAPI (2 μg ml^{-1}) for 5 min. Quantification using our immunohistochemical technique is critically dependent on the stability of the tissue in the first few seconds after application of the DAB–H_2O_2 reaction mix. We found that preincubation of sections with ascorbic acid (1 mM) and DAB for 30 min, before application of the reaction mix, eliminated tissue movement.

Quantification of immunohistochemistry and image processing

Hydrated brain sections were placed in a specially designed microscope stage on a Nikon Diaphot fluorescence microscope. Images of nuclei and GFAP staining were captured via a cooled CCD camera (ORCA-03G, Hamamatsu, Japan) and ImageHopper (Samsara Research, Dorking, UK). Water was removed and replaced with the DAB–H_2O_2 reaction mixture and images in brightfield were captured at 1 s^{-1} over 100 s.

Figure 2*A* shows selected images obtained during the rapid time course of DAB–H_2O_2 reaction product development in *ex vivo* brain section from rats subjected to MCAo (70 min) and 24 h reperfusion. Images of DAB polymer density were subsequently generated by applying Beer–Lambert's Law to the sequence, i.e. the log ratio of the first image to subsequent images, thereby generating an optical density map (Fig. 2*B*). The optical densities through the stack for different regions (red square in Fig. 2*B*) were corrected for DAB–H_2O_2 reaction product development over the lumen of a cerebral microvessel free of tissue (green square in Fig. 2*B*). Time courses for DAB–H_2O_2 product development in tissue, the tissue-free region (blank) and resulting net tissue are shown in Fig. 2*C*. The dotted line represents the regression analysis of the linear portion for net tissue product development over the first 25 s. Optical density values in the stack that fell outside the linear portion were excluded from further analysis. The Nrf2 spatial map shown in Fig. 2*D* was calculated by carrying out a linear regression on the stack of optical density images after subtracting blank values.

The time course of Nrf2 activation after ischaemia-reperfusion injury was examined in core and peri-infarct regions of the stroke-affected hemisphere as well as the contralateral hemisphere. The image in Fig. 3*A* is a composite of the upper left-hand region of the section shown in Fig. 2*A*. GFAP fluorescence staining was used to identify activated astrocytes and to discriminate the infarct core and peri-infarct region in the stroke-affected hemisphere (Fig. 3*A*). Total Nrf2 levels are shown in pseudo-colour in Fig. 3*B*. To quantify the nuclear to cytoplasmic ratios of Nrf2 distribution, we used the DAPI image of nuclei (Fig. 3*C*) and applied a binary mask to segment the Nrf2 image to obtain nuclear Nrf2 content (Fig. 3*D*). A similar binary mask of a 4 μm wide ring around each nucleus (taken to be its cytoplasm) was also applied (Fig. 3*E*), and ratios were then obtained for each nucleus–cytoplasm pair. The cellular Nrf2 content was determined from the weighted mean content of each nucleus–cytoplasm pair and expressed as optical density (OD) increase rate per 1000 s, i.e. $(s \times 10^3)^{-1}$. Stroke regions of the brain were separated into core and periphery based on the intensity of GFAP staining, used as a marker for astrocytic activation.

Culture of murine brain endothelial cell line bEnd.3

The immortalised murine-derived brain endothelial cell line bEnd.3 was purchased from ATCC-LGC (Teddington, UK) and grown in DMEM (Sigma Aldrich) supplemented with 10% fetal bovine serum, 4 mM L-glutamine, 100 U ml^{-1} penicillin G and 100 μg ml^{-1} streptomycin. bEnd.3 cells (passage 9–15) were maintained in a humidified incubator at 37°C and 5% CO_2 and 95% air atmosphere. Cell suspensions were diluted in DMEM and plated onto Superfrost Plus slides for DAB immunohistochemistry. An endothelial phenotype was confirmed

based on immunostaining monolayers for endothelial nitric oxide synthase and von Willebrand factor (Rowlands *et al.* 2011).

Nrf2 content in bEnd.3 cells determined by quantitative immunohistochemistry

bEnd.3 cells were treated for 1–4 h with DMEM containing vehicle (DMSO, 0.01% v/v) and or 2.5 μM D,L-sulforaphane. Cells were fixed, permeabilised and quenched for endogenous peroxidase, avidin and biotin as described previously. Cells were incubated with a rabbit anti-Nrf2 primary antibody for 16 h at 4°C and then with the biotinylated secondary antibody and ABC reagent. DAPI in PBS was used for the identification of cellular nuclei. Stained cells remained hydrated in PBS on the Nikon Diaphot microscope stage and were imaged for nuclei by DAPI fluorescence. PBS was removed and replaced with the DAB–H_2O_2 reaction mix in PBS. Images of the reaction were captured under brightfield at 0.5 s intervals over 50 s and processed to determine nuclear to cytoplasmic distribution of Nrf2 following treatment with sulforaphane.

Statistical analysis

Data denote mean ± SEM of measurements in $n = 3$–5 different animals, with a minimum of three sections analysed per brain in each animal. Data in bEnd.3 cells were obtained from five independent cultures. Analysis of variance (ANOVA) followed by Tukey's *post hoc* test or Student's paired *t* test was applied as appropriate with $P < 0.05$ considered significant.

Results

Initial rate of DAB–H_2O_2 reaction product formation as an index of Nrf2 content in brain tissue sections

When rat brain sections (10 μm), obtained after MCAo (70 min) and 24 h reperfusion, were incubated with an anti-Nrf2 antibody, HRP-conjugated secondary and treated with ABC solution, the DAB–H_2O_2 reaction product formation was linear over the first 25 s (Fig. 2*C*), confirming the initial linear time course of DAB polymer formation in BSA gelatine sections (Fig. 1*A* and *B*). As illustrated in Fig. 3, nuclear to cytoplasmic ratios of Nrf2 distribution were quantified by using the DAPI image of nuclei (Fig. 3*C*) to segment the Nrf2 image (Fig. 3*B*) into nuclear (Fig. 3*D*) and cytoplasmic (Fig. 3*E*) compartments.

Temporal changes in nuclear to cytoplasmic Nrf2 distribution in rat brains following MCAo

The ratio between nuclear to cytoplasmic Nrf2 content after 4 h reperfusion was lower in the stroke-affected than contralateral hemisphere (Fig. 4*D*) and values observed in control brains (Fig 4*A* and *D*). After 24 h reperfusion, there was a significant increase in the mean nuclear to cytoplasmic Nrf2 ratio (>1.0) in the stroke-affected *versus* contralateral hemisphere (Fig. 4*B* and *D*) or control brains (Fig. 4*A* and *D*). Following 72 h reperfusion, Nrf2 ratios in both the stroke-affected and the contralateral hemispheres decreased below values in control brains, and notably Nrf2 ratios were similar in stroke-affected and contralateral regions (Fig. 4*D*).

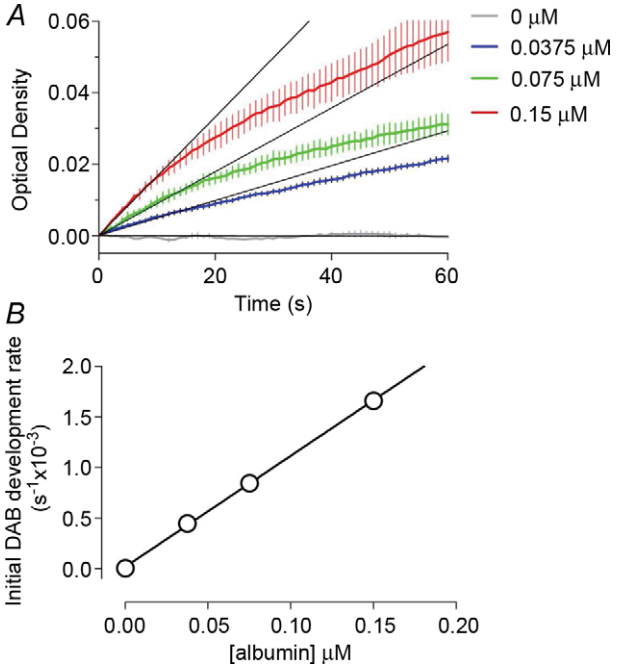

Figure 1. Proof-of-principle experiment that protein content in frozen sections can be quantified from initial rates of DAB–H_2O_2 reaction product formation
Frozen sections (10 μm) of porcine gelatine containing known concentrations of bovine serum albumin (BSA) were incubated with anti-BSA primary antibody, complementary HRP-conjugated secondary antibody and treated with ABC solution. *A*, sequential images of the DAB–H_2O_2 reaction product were captured, optical densities plotted and a regression calculated for the initial linear portion for each BSA concentration. Data denote mean ± SEM of measurements in four frozen gelatine sections for each BSA concentration. *B*, regression coefficients for initial DAB development rate plotted against BSA concentration; mean ± SEM of measurements from four sections for each BSA concentration, noting that standard errors of the regression analyses fall within the symbols.

Temporal changes in total cellular Nrf2 content in stroke and contralateral hemispheres

Immunopositive staining for GFAP, an index of astrocyte activation in the brain, was only just detectable after 4 h reperfusion and increased further after 24 and 72 h reperfusion (data not shown). Figure 5 summarises paired measurements in individual animals of the mean Nrf2 content per cell in stroke and contralateral brain hemispheres following 4, 24 and 72 h reperfusion. Increased GFAP-immunopositive staining detected after 24 and 72 h reperfusion enabled us to define core and peri-infarct regions in the stroke hemisphere. After 4 h reperfusion, the total Nrf2 content per cell was similar in the contralateral hemisphere in control brains, although a significant increase in Nrf2 content was observed in the stroke-affected regions (Fig. 5*A* and *E*). After 24 and 72 h reperfusion, total Nrf2 levels were significantly increased in peri-infarct compared to core regions (Fig. 5*B*, *C* and *E*) of the stroke hemisphere. Notably, the elevated Nrf2 content in the core after 24 h reperfusion (Fig. 5*B*) returned to levels detected in the contralateral hemisphere after 72 h reperfusion (Fig. 5*C* and *E*).

Sulforaphane pretreatment modulates nuclear and total cellular Nrf2 content in the brain after 24 h ischaemia-reperfusion

Treatment of naïve rats with sulforaphane (5 mg kg^{-1} I.P.) had no significant effect on nuclear to cytoplasmic distribution of Nrf2 (Fig 4*A* and *D*) or total cellular Nrf2 content (data not shown) when measured 24 h later. However, pretreatment of animals with sulforaphane 1 h before MCAo and 24 h reperfusion led to a significant decrease in nuclear to cytoplasmic Nrf2 ratios (Fig. 4*C* and *E*) and total Nrf2 content (Fig. 5*D* and *E*) in the stroke-affected and contralateral hemispheres.

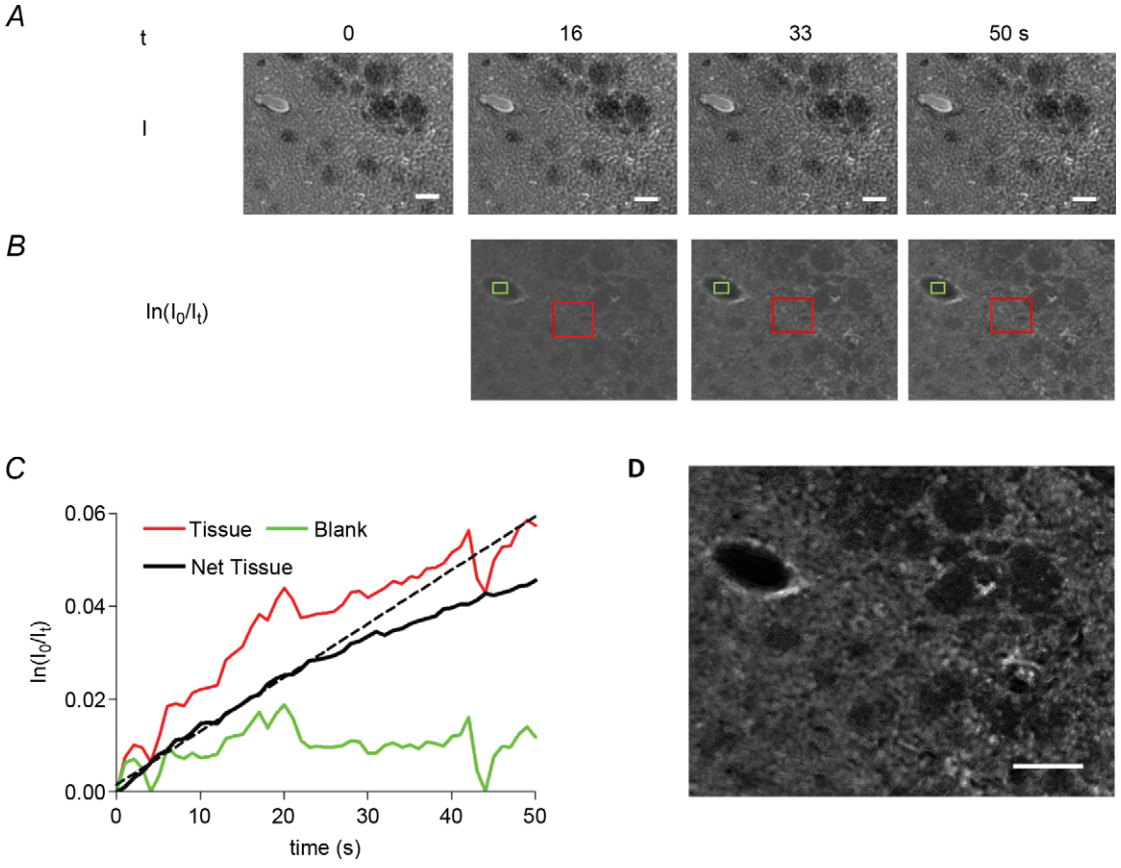

Figure 2. Method for estimating Nrf2 content in a brain tissue section
A, selection of a series of images captured at 1 s^{-1} during incubation with DAB–H_2O_2. *B*, the optical density (OD) calculated on a pixel by pixel basis using the Beer–Lambert law ($\ln(I_o/I_t)$). A region of interest through the image stack over a portion free of tissue (green square) was subtracted from that over the tissue (red square) leaving the HRP-dependent reaction product development. *C*, time courses for tissue, blank (cerebral microvessel lumen) and net tissue DAB–H_2O_2 product formation. The initial rate of DAB–H_2O_2 reaction (dotted line) was assessed from the first 25 s, and the image in *D* formed from a pixel by pixel regression of that initial portion of the stack shown in *B* after subtraction of the blank values. This image was taken to represent levels of Nrf2. Scale bars = 50 μm.

Sulforaphane induces nuclear accumulation of Nrf2 in bEnd.3 brain endothelial cells

To further validate the application of our quantitative DAB–H_2O_2 immunohistochemical technique for cultured brain endothelial cells, we treated bEnd.3 cells with sulforaphane (2.5 μM) for 1–4 h and determined the time course of changes in nuclear to cytoplasmic Nrf2 distribution. Figure 6*A* illustrates representative images of DAB–H_2O_2 reaction product formation in bEnd.3 cells treated for 2 h with sulforaphane, with nuclear to cytoplasmic Nrf2 content in response to vehicle and sulforaphane summarised in Fig. 6*B*. Notably, sulforaphane significantly increased Nrf2 content in nuclear structures after 1–4 h treatment (Fig. 6*C*).

Discussion

We have investigated whether stroke leads to time-dependent changes in the distribution of Nrf2 between the nucleus and surrounding cytoplasm in cells in the brain, and whether pretreatment with the Nrf2 inducer sulforaphane affects the spatial distribution of Nrf2 following cerebral ischaemia-reperfusion injury. Our novel immunohistochemical technique has enabled us to simultaneously quantify the content of the redox sensitive transcription factor Nrf2 in nuclear and cytoplasmic compartments of cells in brain *ex vivo* following reperfusion injury. We report that nuclear to cytoplasmic Nrf2 ratios in stroke-affected regions were initially decreased after 4 h, increased after 24 h and then declined after 72 h reperfusion. Moreover, Nrf2 expression was significantly higher in peri-infarct than in infarct core regions of the stroke-affected hemisphere. Pretreatment of animals with sulforaphane decreased nuclear Nrf2 content in the stroke and contralateral hemispheres, and the total Nrf2 content in peri-infarct and core regions of the stroke-affected hemisphere after 24 h reperfusion. These findings suggest that sulforaphane pretreatment affords protection against oxidative stress and thereby reduces the

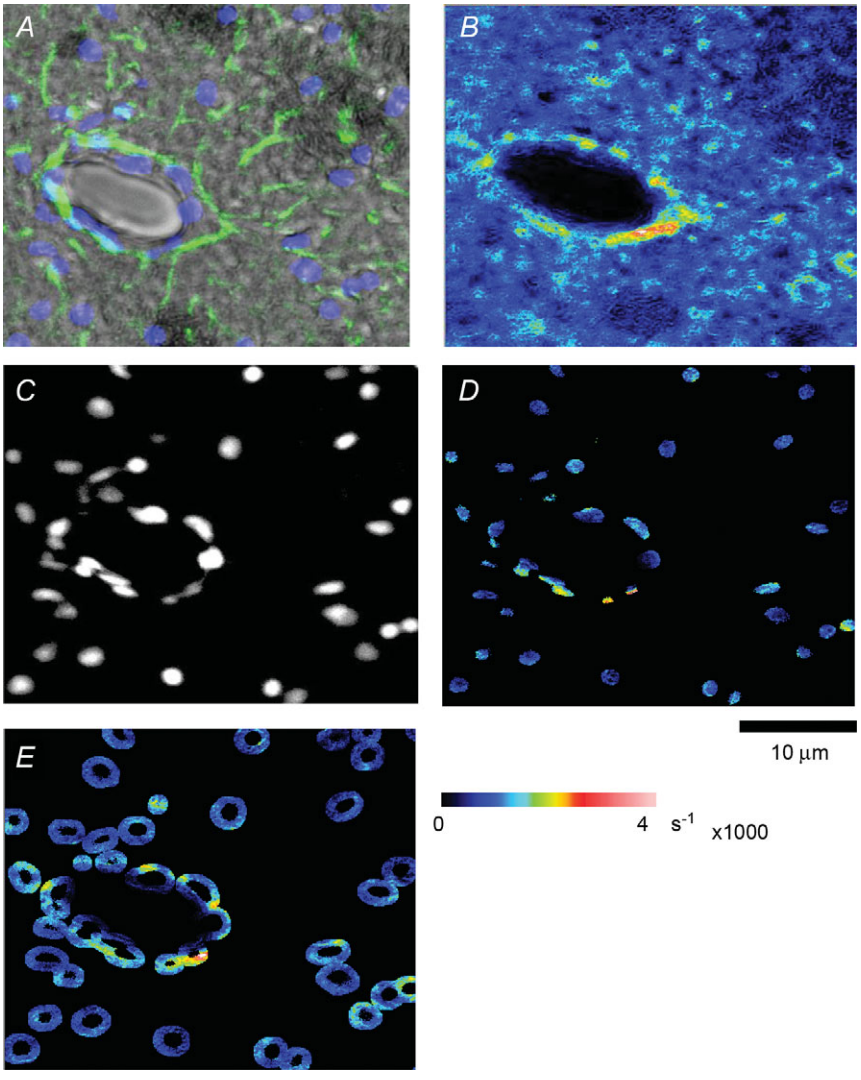

Figure 3. Segmentation to identify Nrf2 content in nuclear and cytoplasmic cellular compartments in the brain following MCAo and 24 h reperfusion
A, composite image of the left-hand portion of the section in Fig. 2*A*, with a fluorescence overlay of nuclei stained with DAPI (blue) and astrocytes with GFAP (green). *B*, Nrf2 image is scaled to a pseudo-colour map. *C*, DAPI image of the nuclei was used to generate a mask that segmented the Nrf2 concentration in nuclei, as shown in *D*. *E*, cytoplasm was taken to be a ring of 4 μm around each nucleus. The combined nucleus and its cytoplasm were taken to represent a cell.

necessity for marked increases in nuclear accumulation of Nrf2 following stroke.

Immunohistochemical techniques involving DAB have predominantly employed the development of DAB polymer for a qualitative analysis of the expression and localisation of proteins of interest in cells using histological stains (Taylor & Levenson, 2006). Immunohistochemical and immunofluorescence techniques currently require

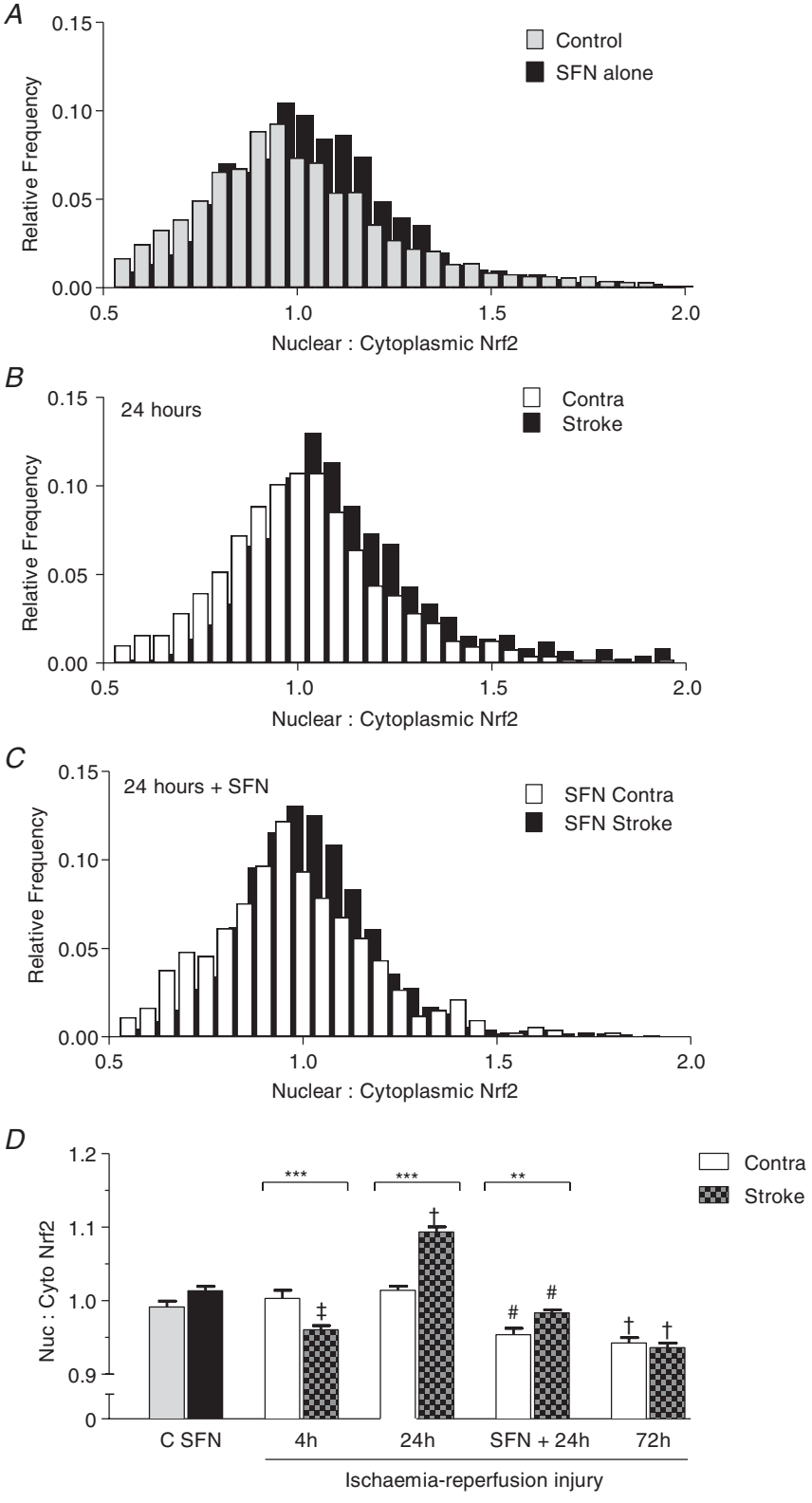

Figure 4. Temporal changes in nuclear to cytoplasmic Nrf2 levels in rat brain following stroke and reperfusion injury
The ratio of Nrf2 content in each nucleus relative to its surrounding cytoplasm was calculated and is displayed in the histograms. *A*, nuclear to cytoplasmic Nrf2 ratios in 3199 cells from five control animals compared to 1869 cells from three animals 24 h after sulforaphane (SFN) treatment. *B*, data from three animals after 24 h reperfusion in stroke (1194 cells) and contralateral hemispheres (1675 cells). *C*, pretreatment with sulforaphane for 1 h followed by MCAo and 24 h reperfusion: stroke hemisphere (2420 cells) *versus* contralateral hemisphere (1273 cells) in three animals. *D*, summary of nuclear to cytoplasmic Nrf2 ratios after MCAo and ischaemia-reperfusion, with additional mean data shown for 4 h reperfusion (2633 cells in stroke *versus* 1580 cells in contralateral hemisphere, $n = 3$ animals) and 72 h reperfusion (1725 cells in stroke *versus* 1168 cells in contralateral hemisphere, $n = 3$ animals). Data denote mean ± SEM. $^{**}P < 0.01$, $^{***}P < 0.001$, $^{\#}P < 0.001$ between contralateral and stroke hemispheres in untreated and SFN treated groups; ‡$P < 0.01$ and †$P < 0.001$ *versus* control brains.

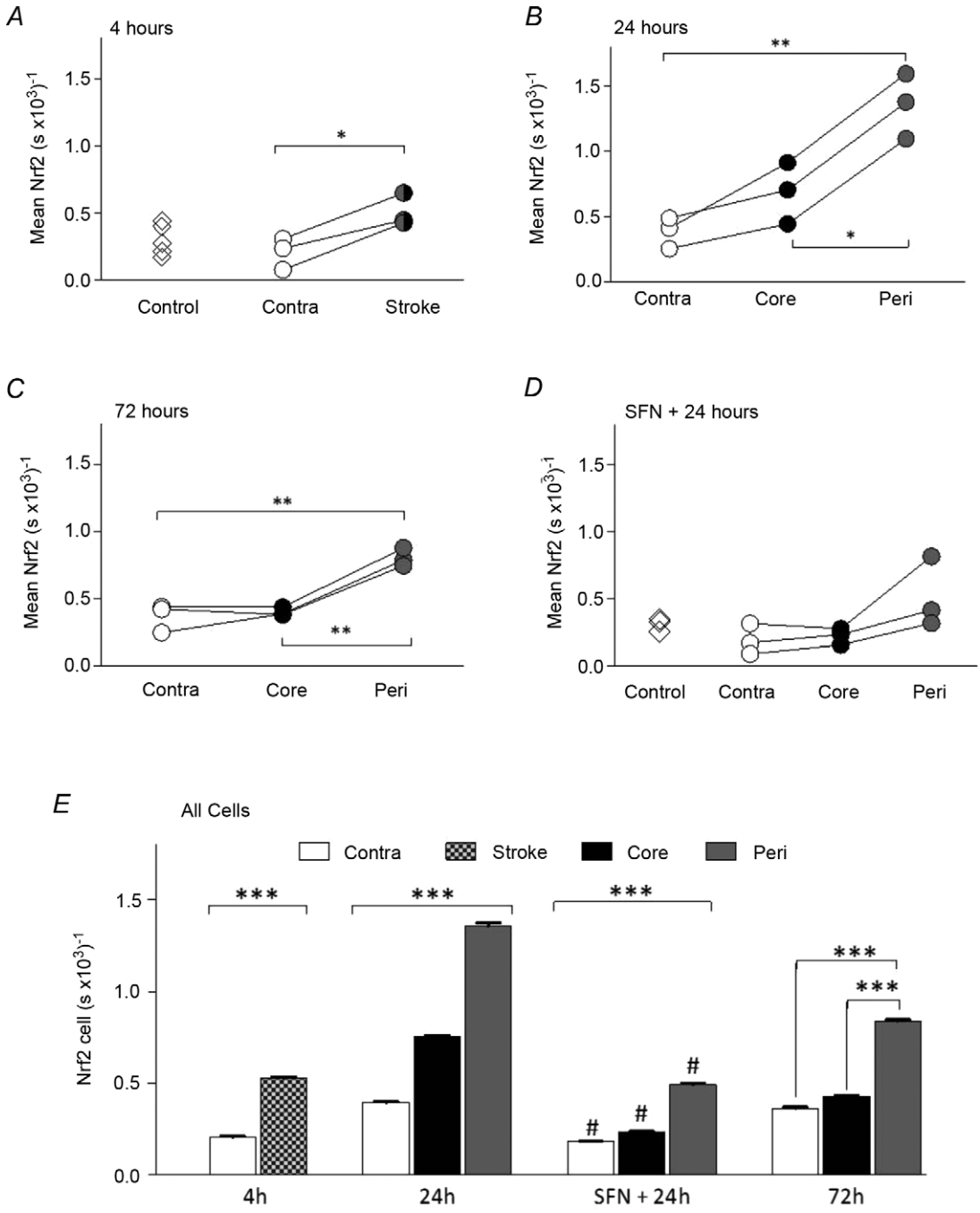

Figure 5. Temporal and spatial changes in total cellular Nrf2 content in brain cells following stroke and reperfusion injury

Total Nrf2 content was calculated on a cellular basis for stroke-affected and contralateral hemispheres in four sets of animals, with additional data showing Nrf2 content in control animals (diamonds in *A*) or sulforaphane-treated animals not undergoing MCAo (diamonds in *D*). Paired comparisons are shown for each animal following 4 h (*A*), 24 h (*B*) and 72 h (*C*) reperfusion, respectively. Total cellular Nfr2 content in core and peri-infarct regions of the stroke hemisphere could only be resolved following 24 and 72 h reperfusion. *D*, effects of sulforaphane pre-treatment on Nrf2 content in core and peri-infarct regions of the stroke hemisphere and contralateral hemisphere following 24 h reperfusion. In *A–D* data denote mean ± SEM. $^{*}P < 0.05$, $^{**}P < 0.01$ and standard errors lie within the symbols. *E*, summary of mean Nrf2 content per cell pooled from different brain regions in all animals following reperfusion. Data denote mean ± SEM, $n = 3$ animals per group. $^{\#}P < 0.001$ for respective regions of sulforaphane pretreated *versus* untreated animals. In the MCAo groups, values for contralateral, core and peri-infarct regions are significantly different from each other, $^{***}P < 0.001$.

sophisticated image analysis software to quantify the degree of staining on a pixel by pixel basis (Matkowskyj *et al.* 2000; Kirkeby & Thomsen, 2005; Montgomery *et al.* 2008). Such methods of quantification, however, provide only semi-quantitative read-outs and do not provide an accurate measure of the protein concentration present in cellular compartments. Measurement of protein in tissues has relied on a combination of immunoblotting of whole tissue homogenates, whereby a global change in the tissue is detected, but information on spatial changes is lost. The novel method described in this study is a development of a technique we previously reported (Gauden *et al.* 2007), where HRP was quantified in brain tissue to obtain permeability–surface area product measurements of cerebrovascular permeability following ischaemia-reperfusion injury. We have advanced this

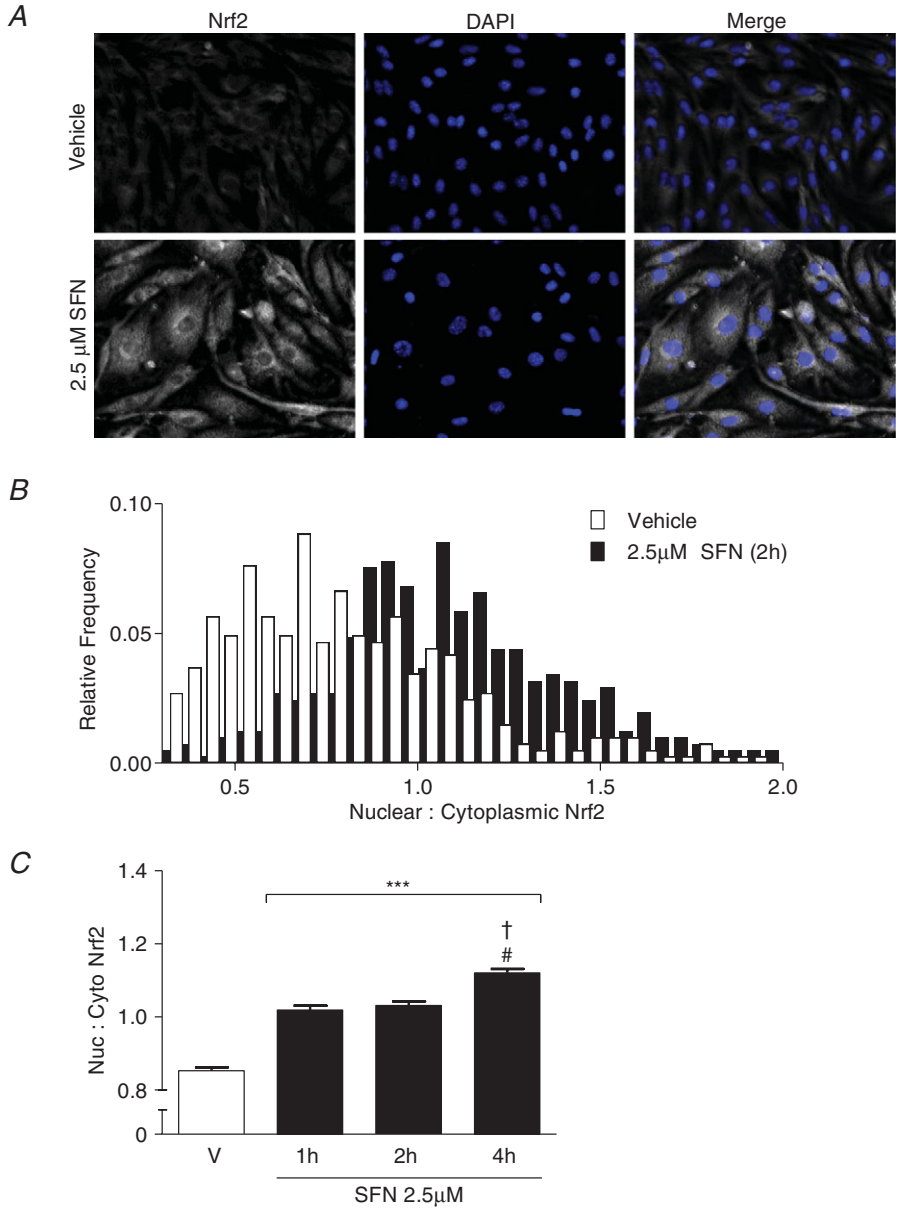

Figure 6. Nuclear distribution of Nrf2 in bEnd.3 endothelial cells following sulforaphane treatment
Confluent bEnd.3 endothelial cells on glass slides were treated for 1–4 h with sulforaphane (SFN, 2.5 μM) and nuclear to cytoplasmic distribution of Nrf2 was analysed by quantitative immunohistochemistry. *A*, images showing DAB–H_2O_2 reactivity map for Nrf2, nuclei identified by DAPI (blue) and a merge for bEnd.3 cells treated with vehicle (upper panel) or sulforaphane (SFN, lower panel) for 2 h. *B*, histogram of nuclear to cytoplasmic ratio of Nrf2 for each respective bEnd.3 cell analysed (106 cells in three different bEnd.3 cultures). *C*, mean nuclear to cytoplasmic ratio of Nrf2 for cells treated with vehicle (V) or SFN for 1, 2, or 4 h. Data denote mean ± SEM, $n = 4$ independent experiments in different bEnd.3 cell cultures. $^{***}P < 0.001$ *versus* vehicle. $^{\#}P < 0.001$ for 1 h *versus* 4 h SFN treatment and †$P < 0.001$ 2 h *versus* 4 h SFN treatment.

technique and here demonstrate that changes in protein concentration, e.g. the redox sensitive transcription factor Nrf2, can be quantified directly with sufficient temporal and spatial resolution to measure the concentration within nuclear and cytoplasmic compartments of cells in the brain.

Activation and nuclear accumulation of Nrf2 upregulates endogenous antioxidant defences to restore cellular redox homeostasis via the induction of phase II defence enzymes and antioxidant stress proteins (Ishii *et al.* 2000, 2004; Motohashi & Yamamoto, 2004; Taguchi *et al.* 2011), yet no information is available on the nuclear to cytoplasmic distribution of Nrf2 in brain tissue following transient ischaemia-reperfusion injury. In our rat MCAo model, we have obtained the first measurements of nuclear to cytoplasmic Nrf2 distribution in both contralateral and stroke-affected hemispheres. We found a decrease in nuclear Nrf2 content in stroke regions after 4 h reperfusion, potentially reflecting an increase in Nrf2 synthesis and greater cytoplasmic content. Nrf2 ratios were increased significantly in stroke regions after 24 h reperfusion, and after 72 h declined in both stroke-affected and contralateral regions to values below those in control brains (Fig. 4*D*). Notably, after 72 h reperfusion, the nuclear to cytoplasmic Nrf2 distribution was similar in stroke-affected and contralateral hemispheres (Fig. 4*D*), suggesting possible export of Nrf2 from the nucleus.

Although phosphorylation of Nrf2 has been reported to affect nuclear translocation of Nrf2 and transcriptional activation of its target antioxidant enzymes, (Niture *et al.* 2011; Chen *et al.* 2012) others have shown that site-directed mutagenesis of Nrf2 at different mitogen-activated protein kinase consensus sites has only a limited effect on Nrf2-dependent gene expression and/or ARE-dependent luciferase activity (Zipper & Mulcahy, 2003; Shen *et al.* 2004; Sun *et al.* 2009). To further validate our polyclonal Nrf2, we compared two different Nrf2 antibodies (see Supplemental Fig. S1) and examined the effects of treating *ex vivo* brain sections with alkaline phosphatase on nuclear/cytoplasmic Nrf2 ratios and total cellular Nrf2 levels (see Supplemental Fig. S2). Notably, similar total and nuclear/cytoplasmic ratios for Nrf2 were measured using the two different Nrf2 antibodies. Furthermore, treatment with alkaline phosphatase had no significant effect on Nrf2 ratios or total cellular Nrf2 content in *ex vivo* brain sections.

In our study a significant increase in total cellular Nrf2 content was observed in peri-infarct region and core regions of the stroke hemisphere after 24 h reperfusion (Fig. 5*B*), which decreased following 72 h reperfusion (Fig. 5*C*). Based on the significantly lower cellular Nrf2 content in the infarct core compared to peri-infarct regions after reperfusion (Fig. 5*E*), we suggest that cells in peri-infarct regions have an elevated antioxidant capacity, enabling them to counteract the stress induced by reactive oxygen species following ischaemia-reperfusion. Previous studies in mice subjected to MCAo have only detected Nrf2 immunopositive cells in the peri-infarct region after 8–72 h reperfusion and, unlike our findings, could not observe Nrf2 staining in the infarct core over this time period (Tanaka *et al.* 2011). More recent studies in rats subjected to MCAo and 24 h reperfusion were also unable to detect Nrf2 immunopositive staining in the infarct core (Dang *et al.* 2012), highlighting the sensitivity of our quantitative immunohistochemical technique.

We found that pretreatment of animals with the Nrf2 inducer sulforaphane prior to MCAo significantly affected nuclear accumulation of Nrf2 (Fig. 4*C* and *D*) and total cellular Nrf2 content (Fig. 5*D* and *E*) in both stroke-affected and contralateral regions after 24 h reperfusion. Previous studies in mice have shown that following intraperitoneal sulforaphane administration, this isothiocyanate rapidly crosses the blood–brain barrier, accumulates in the striatum and cortex within 15 min, and increases Nrf2 protein levels within 1–2 h (Jazwa *et al.* 2011). Furthermore, increased Nrf2 protein levels in the brain induced by sulforaphane are accompanied by an increased expression of its target antioxidant genes HO-1 and NQO1 after 16 h (Jazwa *et al.* 2011), indicating that pretreatment with sulforaphane activates Nrf2 and cellular antioxidant defences in the brain.

Oxidative stress experienced by infarcted areas of the brain upon reperfusion (Dirnagl *et al.* 1995; Peters *et al.* 1998; Yamato *et al.* 2003) results in increased cerebrovascular permeability (Kaya *et al.* 2003; Kahles *et al.* 2007; Woodfin *et al.* 2011). Protective effects of Nrf2 in cerebral ischaemia-reperfusion injury have been reported (Shih *et al.* 2005; Yang *et al.* 2009; Shah *et al.* 2010; Son *et al.* 2010), and notably, post-treatment of the ischaemic brain with inducers of Nrf2, such as curcumin, epicatechin, plumbagin and sulforaphane, reduces the volume of infarcted tissue and oedema formation (Yang *et al.* 2009; Shah *et al.* 2010; Son *et al.* 2010), implying a decrease in cerebrovascular permeability. Moreover, administration of sulforaphane to animals following stroke partially restores neurological and behavioural function (Zhao *et al.* 2007). Activation of Nrf2 in cells *in vitro* has been shown to protect astrocytes and brain endothelial cells (Bell *et al.* 2011; Pan *et al.* 2011; Williamson *et al.* 2012), with sulforaphane enhancing nuclear accumulation of Nrf2 and induction of its downstream phase II detoxification enzyme NQO1 (Kraft *et al.* 2004; Danilov *et al.* 2009). We further validated our immunohistochemical technique for application *in vitro* by examining the effects of sulforaphane on nuclear to cytoplasmic Nrf2 distribution in bEnd.3 brain endothelial cells. In our study, sulforaphane induced nuclear accumulation of Nrf2 in bEnd.3 cells over 1–4 h (Fig. 6), mirroring the time course of Nrf2 expression in the striatum and cortex of mice treated with sulforaphane

in vivo (Jazwa *et al.* 2011). Thus, nuclear accumulation of Nrf2 is modulated by sulforaphane in the brain *in vivo* and in brain endothelial cells *in vitro*.

In Nrf2-deficient mice, experimental stroke is characterised by exacerbated oedema formation and an increased recruitment of pro-inflammatory cells to stroke-affected regions (Shih *et al.* 2005; Yang *et al.* 2009). Nrf2 has been implicated in dampening down pro-inflammatory processes (Li *et al.* 2008), and anti-inflammatory actions of sulforaphane may in part be mediated by inhibition of NF-κB signalling (Heiss *et al.* 2001; Cheung & Kong, 2010; Benedict *et al.* 2012). As treatment with sulforaphane after stroke reduces cerebral infarct volume and oedema formation (Zhao *et al.* 2006), it seems likely that the cytoprotective actions of sulforaphane in the brain involve both activation of Nrf2 and inhibition of pro-inflammatory signalling pathways.

In conclusion, we have developed a novel quantitative DAB–H_2O_2 immunohistochemical technique to analyse temporal and spatial expression of proteins, and in particular transcription factors such as Nrf2, in the brain following stroke and endothelial cells *in vitro*. We have quantified the nuclear to cytoplasmic Nrf2 content in stroke-affected regions and observed a significant increase in the Nrf2 ratio in peri-infarct regions after 24 h reperfusion. To our knowledge, our study is the first to investigate the effects of sulforaphane pretreatment on spatial Nrf2 distribution in the brain following cerebral ischaemia-reperfusion. Rapid accumulation of sulforaphane in the brain and subsequent upregulation of Nrf2 and antioxidant enzymes (Jazwa *et al.* 2011) may reduce the necessity for later adaptive increases in Nrf2 expression following stroke. Importantly, this technique can readily be applied for quantification of nuclear accumulation of other transcription factors, such as NF-κB, HIF-1α, CREB or AP-1, involved in redox signalling in the brain following ischaemic or traumatic insults, in other tissues and in cultured cells *in vitro*. We propose that upregulation of Nrf2 and its target antioxidant genes *prior* to stroke using natural hormetic agents such as sulforaphane and/or other Nrf2 inducers to modulate intracellular redox signalling (Siow & Mann, 2010) affords protection against cerebrovascular oxidative damage.

References

Alfieri A, Srivastava S, Siow RC, Modo M, Fraser PA & Mann GE (2011). Targeting the Nrf2-Keap1 antioxidant defence pathway for neurovascular protection in stroke. *J Physiol* **589**, 4125–4136.

Bell KF, Fowler JH, Al-Mubarak B, Horsburgh K & Hardingham GE (2011). Activation of Nrf2-regulated glutathione pathway genes by ischemic preconditioning. *Oxid Med Cell Longev* **2011**, 689524.

Benedict AL, Mountney A, Hurtado A, Bryan KE, Schnaar RL, Dinkova-Kostova AT & Talalay P (2012). Neuroprotective effects of sulforaphane after contusive spinal cord injury. *J Neurotrauma* **29**, 2576–2586.

Candelario-Jalil E (2009). Injury and repair mechanisms in ischemic stroke: considerations for the development of novel neurotherapeutics. *Curr Opin Investig Drugs* **10**, 644–654.

Chapple SJ, Siow RC & Mann GE (2012). Crosstalk between Nrf2 and the proteasome: therapeutic potential of Nrf2 inducers in vascular disease and aging. *Int J Biochem Cell Biol* **44**, 1315–1320.

Chen H, Yoshioka H, Kim GS, Jung JE, Okami N, Sakata H, Maier CM, Narasimhan P, Goeders CE & Chan PH (2011). Oxidative stress in ischemic brain damage: mechanisms of cell death and potential molecular targets for neuroprotection. *Antioxid Redox Signal* **14**, 1505–1517.

Chen HH, Chen YT, Huang YW, Tsai HJ & Kuo CC (2012). 4-Ketopinoresinol, a novel naturally occurring ARE activator, induces the Nrf2/HO-1 axis and protects against oxidative stress-induced cell injury via activation of PI3K/AKT signalling. *Free Radic Biol Med* **52**, 1054–1066.

Cheung KL & Kong AN (2010). Molecular targets of dietary phenethyl isothiocyanate and sulforaphane for cancer chemoprevention. *AAPS J* **12**, 87–97.

Dang J, Brandenburg LO, Rosen C, Fragoulis A, Kipp M, Pufe T, Beyer C & Wruck CJ (2012). Nrf2 expression by neurons, astroglia, and microglia in the cerebral cortical penumbra of ischemic rats. *J Mol Neurosci* **46**, 578–584.

Danilov CA, Chandrasekaran K, Racz J, Soane L, Zielke C & Fiskum G (2009). Sulforaphane protects astrocytes against oxidative stress and delayed death caused by oxygen and glucose deprivation. *Glia* **57**, 645–656.

Dinkova-Kostova AT & Kostov RV (2012). Glucosinolates and isothiocyanates in health and disease. *Trends Mol Med* **18**, 337–347.

Dirnagl U, Iadecola C & Moskowitz MA (1999). Pathobiology of ischaemic stroke: an integrated view. *Trends Neurosci* **22**, 391–397.

Dirnagl U, Lindauer U, Them A, Schreiber S, Pfister HW, Koedel U, Reszka R, Freyer D & Villringer A (1995). Global cerebral ischemia in the rat: online monitoring of oxygen free radical production using chemiluminescence in vivo. *J Cereb Blood Flow Metab* **15**, 929–940.

Fraser PA (2011). The role of free radical generation in increasing cerebrovascular permeability. *Free Radic Biol Med* **51**, 967–977.

Gauden V, Hu DE, Kurokawa T, Sarker MH & Fraser PA (2007). Novel technique for estimating cerebrovascular permeability demonstrates capsazepine protection following ischemia-reperfusion. *Microcirculation* **14**, 767–778.

Graham RC Jr & Karnovsky MJ (1966). The early stages of absorption of injected horseradish peroxidase in the proximal tubules of mouse kidney: ultrastructural cytochemistry by a new technique. *J Histochem Cytochem* **14**, 291–302.

Heiss E, Herhaus C, Klimo K, Bartsch H & Gerhauser C (2001). Nuclear factor kB is a molecular target for sulforaphane-mediated anti-inflammatory mechanisms. *J Biol Chem* **276**, 32008–32015.

Iadecola C & Anrather J (2011). Stroke research at a crossroad: asking the brain for directions. *Nat Neurosci* **14**, 1363–1368.

Ikonomidou C & Kaindl AM (2011). Neuronal death and oxidative stress in the developing brain. *Antioxid Redox Signal* **14**, 1535–1550.

Ishii T, Itoh K, Ruiz E, Leake DS, Unoki H, Yamamoto M & Mann GE (2004). Role of Nrf2 in the regulation of CD36 and stress protein expression in murine macrophages: activation by oxidatively modified LDL and 4-hydroxynonenal. *Circ Res* **94**, 609–616.

Ishii T, Itoh K, Takahashi S, Sato H, Yanagawa T, Katoh Y, Bannai S & Yamamoto M (2000). Transcription factor Nrf2 coordinately regulates a group of oxidative stress-inducible genes in macrophages. *J Biol Chem* **275**, 16023–16029.

Itoh K, Mimura J & Yamamoto M (2010). Discovery of the negative regulator of Nrf2, Keap1: a historical overview. *Antioxid Redox Signal* **13**, 1665–1678.

Jazwa A, Rojo AI, Innamorato NG, Hesse M, Fernandez-Ruiz J & Cuadrado A (2011). Pharmacological targeting of the transcription factor Nrf2 at the basal ganglia provides disease modifying therapy for experimental parkinsonism. *Antioxid Redox Signal* **14**, 2347–2360.

Kahles T, Luedike P, Endres M, Galla HJ, Steinmetz H, Busse R, Neumann-Haefelin T & Brandes RP (2007). NADPH oxidase plays a central role in blood–brain barrier damage in experimental stroke. *Stroke* **38**, 3000–3006.

Kam KY, Yu SJ, Jeong N, Hong JH, Jalin AM, Lee S, Choi YW, Lee CK & Kang SG (2011). *p*-Hydroxybenzyl alcohol prevents brain injury and behavioral impairment by activating Nrf2, PDI, and neurotrophic factor genes in a rat model of brain ischemia. *Mol Cells* **31**, 209–215.

Kaya M, Kalayci R, Kucuk M, Arican N, Elmas I, Kudat H & Korkut F (2003). Effect of losartan on the blood–brain barrier permeability in diabetic hypertensive rats. *Life Sci* **73**, 3235–3244.

Kirkeby S & Thomsen CE (2005). Quantitative immunohistochemistry of fluorescence labelled probes using low-cost software. *J Immunol Methods* **301**, 102–113.

Kolominsky-Rabas PL, Heuschmann PU, Marschall D, Emmert M, Baltzer N, Neundorfer B, Schoffski O & Krobot KJ (2006). Lifetime cost of ischemic stroke in Germany: results and national projections from a population-based stroke registry: the Erlangen Stroke Project. *Stroke* **37**, 1179–1183.

Kraft AD, Johnson DA & Johnson JA (2004). Nuclear factor E2-related factor 2-dependent antioxidant response element activation by *tert*-butylhydroquinone and sulforaphane occurring preferentially in astrocytes conditions neurons against oxidative insult. *J Neurosci* **24**, 1101–1112.

Kwak MK, Itoh K, Yamamoto M & Kensler TW (2002). Enhanced expression of the transcription factor Nrf2 by cancer chemopreventive agents: role of antioxidant response element-like sequences in the nrf2 promoter. *Mol Cell Biol* **22**, 2883–2892.

Li W, Khor TO, Xu C, Shen G, Jeong WS, Yu S & Kong AN (2008). Activation of Nrf2-antioxidant signalling attenuates NFkB-inflammatory response and elicits apoptosis. *Biochem Pharmacol* **76**, 1485–1489.

Matkowskyj KA, Schonfeld D & Benya RV (2000). Quantitative immunohistochemistry by measuring cumulative signal strength using commercially available software Photoshop and Matlab. *J Histochem Cytochem* **48**, 303–312.

Modo M, Stroemer RP, Tang E, Veizovic T, Sowniski P & Hodges H (2000). Neurological sequelae and long-term behavioural assessment of rats with transient middle cerebral artery occlusion. *J Neurosci Methods* **104**, 99–109.

Montgomery JD, Hensler HR, Jacobson LP & Jenkins FJ (2008). Validation of a low cost computer-based method for quantification of immunohistochemistry-stained sections. *Appl Immunohistochem Mol Morphol* **16**, 400–404.

Motohashi H & Yamamoto M (2004). Nrf2-Keap1 defines a physiologically important stress response mechanism. *Trends Mol Med* **10**, 549–557.

Nakane PK & Pierce GB Jr (1967). Enzyme-labelled antibodies for the light and electron microscopic localization of tissue antigens. *J Cell Biol* **33**, 307–318.

Niture SK, Jain AK, Shelton PM & Jaiswal AK (2011). Src subfamily kinases regulate nuclear export and degradation of transcription factor Nrf2 to switch off Nrf2-mediated antioxidant activation of cytoprotective gene expression. *J Biol Chem* **286**, 28821–28832.

Ozkul A, Akyol A, Yenisey C, Arpaci E, Kiylioglu N & Tataroglu C (2007). Oxidative stress in acute ischemic stroke. *J Clin Neurosci* **14**, 1062–1066.

Pan H, Wang H, Zhu L, Mao L, Qiao L & Su X (2011). Depletion of Nrf2 enhances inflammation induced by oxyhemoglobin in cultured mice astrocytes. *Neurochem Res* **36**, 2434–2441.

Peters O, Back T, Lindauer U, Busch C, Megow D, Dreier J & Dirnagl U (1998). Increased formation of reactive oxygen species after permanent and reversible middle cerebral artery occlusion in the rat. *J Cereb Blood Flow Metab* **18**, 196–205.

Rowlands DJ, Chapple S, Siow RC & Mann GE (2011). Equol-stimulated mitochondrial reactive oxygen species activate endothelial nitric oxide synthase and redox signalling in endothelial cells: roles for F-actin and GPR30. *Hypertension* **57**, 833–840.

Shah ZA, Li RC, Ahmad AS, Kensler TW, Yamamoto M, Biswal S & Dore S (2010). The flavanol (–)-epicatechin prevents stroke damage through the Nrf2/HO1 pathway. *J Cereb Blood Flow Metab* **30**, 1951–1961.

Shah ZA, Li RC, Thimmulappa RK, Kensler TW, Yamamoto M, Biswal S & Dore S (2007). Role of reactive oxygen species in modulation of Nrf2 following ischemic reperfusion injury. *Neuroscience* **147**, 53–59.

Shen G, Hebbar V, Nair S, Xu C, Li W, Lin W, Keum YS, Han J, Gallo MA & Kong AN (2004). Regulation of Nrf2 transactivation domain activity. The differential effects of mitogen-activated protein kinase cascades and synergistic stimulatory effect of Raf and CREB-binding protein. *J Biol Chem* **279**, 23052–23060.

Shih AY, Imbeault S, Barakauskas V, Erb H, Jiang L, Li P & Murphy TH (2005). Induction of the Nrf2-driven antioxidant response confers neuroprotection during mitochondrial stress *in vivo*. *J Biol Chem* **280**, 22925–22936.

Shohami E, Beit-Yannai E, Horowitz M & Kohen R (1997). Oxidative stress in closed-head injury: brain antioxidant capacity as an indicator of functional outcome. *J Cereb Blood Flow Metab* **17**, 1007–1019.

Siow RC & Mann GE (2010). Dietary isoflavones and vascular protection: activation of cellular antioxidant defenses by SERMs or hormesis? *Mol Aspects Med* **31**, 468–477.

Son TG, Camandola S, Arumugam TV, Cutler RG, Telljohann RS, Mughal MR, Moore TA, Luo W, Yu QS, Johnson DA, Johnson JA, Greig NH & Mattson MP (2010). Plumbagin, a novel Nrf2/ARE activator, protects against cerebral ischemia. *J Neurochem* **112**, 1316–1326.

Sun Z, Huang Z & Zhang DD (2009). Phosphorylation of Nrf2 at multiple sites by MAP kinases has a limited contribution in modulating the Nrf2-dependent antioxidant response. *PLoS ONE* **4**, e6588.

Taguchi K, Motohashi H & Yamamoto M (2011). Molecular mechanisms of the Keap1-Nrf2 pathway in stress response and cancer evolution. *Genes Cells* **16**, 123–140.

Tanaka N, Ikeda Y, Ohta Y, Deguchi K, Tian F, Shang J, Matsuura T & Abe K (2011). Expression of Keap1-Nrf2 system and antioxidative proteins in mouse brain after transient middle cerebral artery occlusion. *Brain Res* **1370**, 246–253.

Taylor CR & Levenson RM (2006). Quantification of immunohistochemistry–issues concerning methods, utility and semiquantitative assessment II. *Histopathology* **49**, 411–424.

Thompson D, Edelsberg J, Colditz GA, Bird AP & Oster G (1999). Lifetime health and economic consequences of obesity. *Arch Intern Med* **159**, 2177–2183.

Toyokuni S, Tanaka T, Hattori Y, Nishiyama Y, Yoshida A, Uchida K, Hiai H, Ochi H & Osawa T (1997). Quantitative immunohistochemical determination of 8-hydroxy-2′-deoxyguanosine by a monoclonal antibody N45.1: its application to ferric nitrilotriacetate-induced renal carcinogenesis model. *Lab Invest* **76**, 365–374.

Williamson TP, Johnson DA & Johnson JA (2012). Activation of the Nrf2-ARE pathway by siRNA knockdown of Keap1 reduces oxidative stress and provides partial protection from MPTP-mediated neurotoxicity. *Neurotoxicology* **33**, 272–279.

Woodfin A, Hu DE, Sarker M, Kurokawa T & Fraser P (2011). Acute NADPH oxidase activation potentiates cerebrovascular permeability response to bradykinin in ischemia-reperfusion. *Free Radic Biol Med* **50**, 518–524.

Yamato S, Kobayashi K, Ebara K, Shimada K & Ohta S (2003). High performance liquid chromatographic determination of acetoacetate by post-column derivatization with *p*-nitrobenzene diazonium fluoroborate. *Biol Pharm Bull* **26**, 397–400.

Yang C, Zhang X, Fan H & Liu Y (2009). Curcumin upregulates transcription factor Nrf2, HO-1 expression and protects rat brains against focal ischemia. *Brain Res* **1282**, 133–141.

Zhang Y, Talalay P, Cho CG & Posner GH (1992). A major inducer of anticarcinogenic protective enzymes from broccoli: isolation and elucidation of structure. *Proc Natl Acad Sci U S A* **89**, 2399–2403.

Zhao J, Kobori N, Aronowski J & Dash PK (2006). Sulforaphane reduces infarct volume following focal cerebral ischemia in rodents. *Neurosci Lett* **393**, 108–112.

Zhao X, Sun G, Zhang J, Strong R, Dash PK, Kan YW, Grotta JC & Aronowski J (2007). Transcription factor Nrf2 protects the brain from damage produced by intracerebral hemorrhage. *Stroke* **38**, 3280–3286.

Zipper LM & Mulcahy RT (2003). Erk activation is required for Nrf2 nuclear localization during pyrrolidine dithiocarbamate induction of glutamate cysteine ligase modulatory gene expression in HepG2 cells. *Toxicol Sci* **73**, 124–134.

Additional information

Competing interests

None.

Author contributions

S.S. conducted the immunohistochemical experiments and analysis of DAB polymer formation in *ex vivo* brain sections. A.A. conducted all MCAo and pharmacological interventions. G.E.M., S.S., A.A., R.C.M.S. and P.A.F. contributed to the design of experiments and drafting of the manuscript. G.E.M. and P.A.F. are the guarantors of this work and assume full responsibility for the integrity of the experimental data and analysis.

Funding

We gratefully acknowledge the support of the British Heart Foundation (FS/09/056) and The Henry Smith Charity (RG20092511).